

# Sulfinylimine Radical in Azido-CDP- and Azido-UDP-Inhibited Ribonucleotide Reductase

Leif A. Eriksson

Contribution from the Department of Quantum Chemistry, Uppsala University, Box 518, S-751 20 Uppsala, Sweden

Received October 29, 1997

**Abstract:** The equilibrium geometry and protonation state of a model of the sulfinylimine type radical observed in the reaction between the modified substrate 2'-azido-2'-deoxyribonucleotide-5'-diphosphate and a cysteine radical at the active site of ribonucleotide reductase (RNR) are investigated by means of hybrid and gradient-corrected density functional theory. The results indicate that the radical is nonplanar and either neutral or anionic. The calculated nitrogen and  $\beta$ -proton hyperfine couplings are highly similar for both these systems and agree very closely with the experimentally observed main couplings of 25 G for  $^{14}\text{N}$  and 8–9 or 6.5 G for  $^1\text{H}_\beta$  (depending on RNR source). The experimental data available at present are hence insufficient for a unique determination of the radical protonation state. It is proposed that  $^{13}\text{C}$  labeling of the cysteine residue in question will provide a unique determination of the protonation state of the radical.

## Introduction

Ribonucleotide reductase (RNR) catalyzes the fundamental reaction of converting ribonucleotides into their deoxyribose counterparts. The enzyme is of high interest in many respects. It contains the first detected stable amino acid radical (Tyr122 in the R2 subunit of *Escherichia coli* RNR),<sup>1</sup> linked via a 35 Å long hydrogen-bonded sequence of amino acids to the active site located in the R1 subunit.<sup>2–4</sup> The neutral tyrosine radical is located in the vicinity of an  $\text{Fe}_2\text{O}_2$  center that structurally, but, as far as is known today, not functionally, strongly resembles the catalytically active diiron complex of methane monooxygenase (MMO).<sup>5</sup>

The reaction center of R1–RNR contains three cysteine residues and one glycine, all of which are essential for the catalytic activity.<sup>2–4,6</sup> A key step in the reaction sequence is the initial creation of a cysteine radical R–S\* at Cys439 in the R1 subunit, via radical transfer from the well-protected Tyr radical in the R2 subunit. The cysteine radical thus created is believed to extract a hydrogen from the ribose sugar ring of the substrate, thereby initiating the ribose to deoxyribose conversion. After completed reaction, radical transfer again occurs from Cys439(R1) to Tyr122(R2), thus restoring the enzyme and protecting its reactive functionality.

Although there is now substantial indirect experimental and theoretical evidence for the proposed radical transfer mechanism,<sup>2,3,6</sup> none of the cysteine-based radicals at the active site

have to date been reported. Very recently, however, spectroscopic evidence has been provided, indicating the existence of a sugar-based radical intermediate.<sup>7</sup> Prior to that the only way to generate an observable radical at the active site has been by subjecting the protein to the modified substrate 2'-azido-2'-deoxyribonucleotide-5'-diphosphate (using cytosine or uracil as base).<sup>8–10</sup> This leads to the appearance of a new radical spectrum, and the simultaneous decay of the tyrosyl radical spectrum and irreversible loss of enzyme activity. Concomitant with the formation of the new radical is also the formation of  $\text{N}_2$ , indicating that the radical is of the imine type.

Several reaction mechanisms and radical intermediates obtained from exposure of RNR to azido-CDP or azido-UDP have been proposed.<sup>8–10</sup> On the basis of careful electron paramagnetic resonance (EPR) and electron spin-echo envelope modulation (ESEEM) measurements, as well as isotope substitution experiments and mutagenesis studies, Salowe et al.<sup>9</sup> and Behravan et al.<sup>10</sup> have proposed that the radical is of the sulfinylimine type (R–S–N–(H)\*), and located at the C225 residue. The reaction mechanism of the azido substrate with the active site of RNR is schematically outlined in Figure 1. Two main hyperfine components have been identified,  $A(^{14}\text{N}) = 25 \text{ G}$  and  $A(^1\text{H}) = 8–9 \text{ G}$ , in mouse RNR<sup>10</sup> (6.5 G in *E. coli* RNR<sup>9</sup>). The existence of only one  $\beta$ -proton coupling has been taken as evidence that the structure is rotated about the C–S bond such that one of the  $\beta$ -protons falls in the C–S–N plane, thereby rendering a near-zero hyperfine tensor for this atom. This is caused by the fact that the unpaired electron of the radical is localized mainly to the S–N  $\pi$ -orbital perpendicular to the molecular (C–S–N) plane. Due to the nodal plane of the  $\pi$ -orbital, the relative orientation of the  $\beta$ -protons to this plane

(1) Ehrenberg, A.; Reichart, P. *J. Biol. Chem.* **1972**, *247*, 3485. Sjöberg, B.-M.; Reichart, P.; Gräslund, A.; Ehrenberg, A.; *J. Biol. Chem.* **1978**, *253*, 6863.

(2) Stubbe, J. A. *Annu. Rev. Biochem.* **1989**, *58*, 257.

(3) Gräslund, A.; Sahlin, M. *Annu. Rev. Biophys. Biomol. Struct.* **1996**, *25*, 259. Sjöberg, B.-M. In *Nucleic Acids and Molecular Biology*, Vol. 9; Eckstein, F., Lilley, D. M. J., Eds.; Springer-Verlag: Berlin, 1995.

(4) Nordlund, P.; Eklund, H. *J. Mol. Biol.* **1993**, *232*, 123. Uhlin, U.; Eklund, H. *Nature* **1994**, *370*, 533. Eriksson, M.; Uhlin, U.; Ramaswamy, S.; Ekberg, M.; Regnström, K.; B.-M. Sjöberg Eklund, H. *Structure* **1997**, *5*, 1077.

(5) Rosenzweig, A. C.; Frederick, C. A.; Lippard, S. J.; Nordlund, P. *Nature* **1993**, *336*, 537.

(6) Siegbahn, P. E. M. *J. Am. Chem. Soc.*, submitted for publication.

(7) Persson, A. L.; Eriksson, M.; Katterle, B.; Pötsch, S.; Sahlin, M.; Sjöberg, B.-M. *J. Biol. Chem.* **1997**, *272*, 31533.

(8) Thelander, L.; Larsson, B.; Hobbs, J.; Eckstein, F. *J. Biol. Chem.* **1976**, *251*, 1398.

(9) Salowe, S.; Bolinger, J. M., Jr.; Ator, M.; Stubbe, J.; McCracken, J.; Peisach, J.; Samano, M. C.; Robins, M. J. *Biochemistry* **1993**, *32*, 12749.

(10) Behravan, G.; Sen, S.; Rova, U.; Thelander, L.; Eckstein, F.; Gräslund, A. *Biochim. Biophys. Acta* **1995**, *1264*, 323.

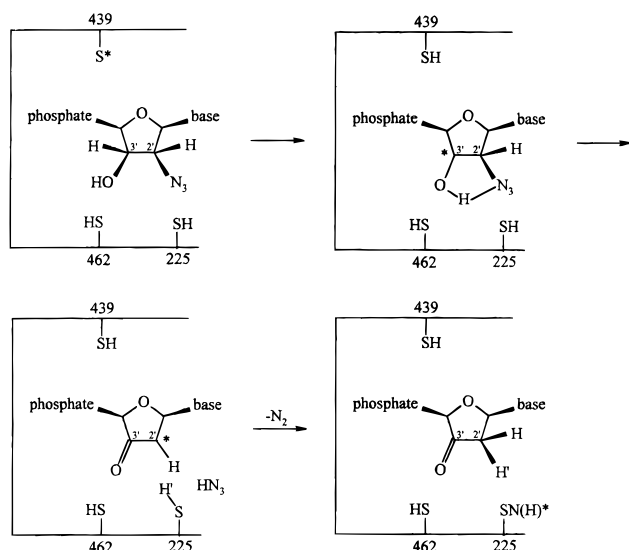


**Figure 1.** Schematic overview of the reaction between the azido substrate and (*E. coli*) RNR, leading to the formation of the sulfinylimine type radical at the C225 residue (adapted from refs 9 and 10).

strongly affects the orbital interaction and hence the amount of induced hyperfine structure, and is a common feature in  $\pi$ -radicals.

We have in the present work conducted detailed density functional theory (DFT) based calculations of different conformers and protonation levels of a model sulfinylimine radical ( $\text{CH}_3\text{-CH}_2\text{-S-N-(H)}^*$ ), to investigate if the radical is of the sulfinylimine type (i), and if so, what its geometrical structure (ii) and protonation state (iii) are.

### Theoretical Approach

The methodological scheme employed has previously been tested and applied in extensive studies of bioradicals, and is known to yield geometries, energetics, and hyperfine properties of very high accuracy.<sup>11–13</sup> All systems are optimized at the B3LYP/6-311G(d,p) level, using the Gaussian 94 program.<sup>14</sup> Vibrational frequency calculations are performed on all the optimized structures, to ensure that these correspond to local minima on the respective potential energy surfaces (PESs). Subsequent calculations are performed at the PWP86/IGLO-III level using the deMon code,<sup>15</sup> for accurate evaluation of the radical hyperfine parameters. We primarily focus on the diagonalized full hyperfine tensors **A**; the corresponding isotropic hyperfine coupling constants (HFCCs) can easily be obtained by extracting  $(1/3)\text{Tr}\{\mathbf{A}\}$  from these. A study of the R–S–N–H rotational energy surface of the neutral radical was

(11) Eriksson, L. A. *Mol. Phys.* **1997**, *91*, 827.

(12) Himo, F.; Gräslund, A.; Eriksson, L. A. *Biophys. J.* **1997**, *72*, 1556.

(13) Eriksson, L. A.; Himo, F. *Res. Trends Phys. Chem.* **1997**, *6*, 153.

(14) Gaussian 94 (Revision E.2): Frisch, M. J.; Trucks, G. W.; Schlegel, H. B.; Gill, P. M. W.; Johnson, B. G.; Robb, M. A.; Cheeseman, J. R.; Keith, T. A.; Peterson, G. A.; Montgomery, J. A.; Raghavachari, K.; Al-Laham, M. A.; Zakrzewski, V. G.; Ortiz, J. V.; Foresman, J. B.; Cioslowski, J.; Stefanov, B. B.; Nanayakkara, A.; Challacombe, M.; Peng, C. Y.; Ayala, P. Y.; Chen, W.; Wong, M. W.; Andres, J. L.; Replogle, E. S.; Gomperts, R.; Martin, R. L.; Fox, D. J.; Binkley, J. S.; Defrees, D. J.; Baker, J.; Stewart, J. P.; Head-Gordon, M.; Gonzalez, C.; Pople, J. A., Gaussian Inc., Pittsburgh, PA, 1995.

(15) St-Amant, A.; Salahub, D. R. *Chem. Phys. Lett.* **1990**, *169*, 387. St-Amant, A. Ph.D. Thesis, Université de Montréal, 1991. Salahub, D. R.; Fournier, R.; Mlynarski, P.; Papai, I.; St-Amant, A.; Ushio, J. J. In *Density Functional Methods in Chemistry*; Labanowski, J., Andzelm, J., Eds.; Springer-Verlag: New York, 1991. Daul, C.; Goursot, A.; Salahub, D. R. In *Grid Methods in Atomic and Molecular Quantum Calculations*; Cerjan, C., Ed.; Nato ASI C142; 1993.

also conducted at the B3LYP/6-311G(d,p) level, from which relative energies and isotropic HFCCs were extracted. For more detailed accounts of radical hyperfine properties within the DFT framework, we refer the reader to refs 16–18.

### Results and Discussion

The optimized geometries corresponding to local minima of the different sulfinylimine radicals are listed in Table 1, along with their relative energies, and in Figure 2 we display schematic structures and spin density distributions for the lowest lying conformers in each protonation class. Three protonation states were investigated; the radical anion ( $\text{CH}_3\text{-CH}_2\text{-S-N}^-$ ), the neutral system ( $\text{CH}_3\text{-CH}_2\text{-S-NH}$ ), and the radical cation ( $\text{CH}_3\text{-CH}_2\text{-S-NH}_2^+$ ), and for each system we investigated both fully planar all-trans conformers, and systems with a nonplanar (twisted) C–C–S–N molecular framework. For the neutral system, we have considered both cis and trans orientations of the imino proton. Both the neutral and the anionic forms of the radical prefer to be in nonplanar orientations, in agreement with the above-mentioned requirements for the observed single  $\beta$ -proton coupling. For the neutral case, the systems with a trans orientation of the imino proton lie ca. 2.5 kcal/mol lower in energy than the corresponding cis conformers. In the case of the cation radical, the planar and twisted structures lie very close in energy, with the planar structure slightly lower. The effects on the geometrical parameters due to the rotational motion are very small for all systems investigated. We also note that, for the twisted radical anion, the torsional angle of the molecular framework (C–C–S–N) is roughly half the value of the corresponding neutral and cationic systems.

The charge distributions display a consecutive transfer of charge upon increased level of protonation, in that the N atom becomes less negative and the sulfur increasingly positive in the series anion–neutral–cation. For the anion, the nitrogen atom carries the main fraction of the negative charge (−0.87), whereas the sulfur is slightly positive (+0.24). For the neutral radicals the charges on N and S are −0.64 and +0.47, respectively, whereas for the cation radicals the Mulliken populations predict the charges −0.38 on N and +0.67 on S. The spin distribution, on the other hand, is highly similar between the neutral and the anionic systems, but deviates more for the cationic radicals. The total ( $\sigma + \pi$ ) unpaired spin populations are listed in Figure 2. The variation in spin density and the orbital interactions are clearly reproduced in the hyperfine HFCCs listed in Table 2. The singly occupied orbital (SOMO) has mainly p-character at the N center, but a stronger s-contribution at sulfur. Hence, the absolute magnitude of  $A_{\text{iso}}(\text{S})$ , which is a direct measure of the unpaired s-orbital spin density at the nucleus, follows the spin density perfectly (5, 4, and 10 G vs spin density 0.30, 0.24, and 0.66). For N, however, there is very little s-character of the SOMO, and thus  $A_{\text{iso}}$  remains more or less unaltered at 4–5 G. For both atoms the anisotropic tensors also follow the trends such that we see an increase in tensor components on S and a decrease on N in the sequence anion–neutral–cation.

Despite the small value of the C–C–S–N torsional angle of the anion (31°), the hyperfine couplings of the two  $\beta$ -protons

(16) Malkin, V. G.; Malkina, O. L.; Eriksson, L. A.; Salahub, D. R. In *Theoretical and Computational Chemistry, Vol. 2, Modern Density Functional Theory—A Tool for Chemistry*; Politzer, P., Seminario, J. M., Eds.; Elsevier: New York, 1995; p 273.

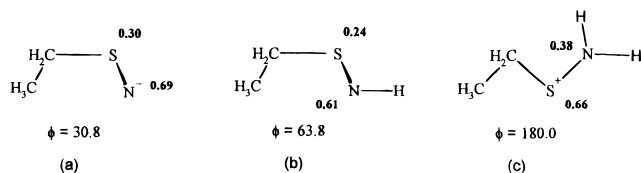
(17) Barone, V. In *Recent Advances in Density Functional Theory, Part 1*; Chong, D. P., Ed.; World Scientific: Singapore, 1995; p 287.

(18) Engels, B.; Eriksson, L. A.; Lunell, S. *Adv. Quantum Chem.* **1996**, *27*, 298.

**Table 1.** Optimized Geometries (Å and deg) and Relative Energies (kcal/mol) of the Different Sulfinylimine Radicals Investigated in This Study<sup>a</sup>

	R-S-N <sup>-</sup>		t-R-S-N-H		c-R-S-N-H		R-S-N-H <sub>2</sub> <sup>+</sup>	
	planar	twisted	planar	twisted	planar	twisted	planar	twisted
R(C <sub>α</sub> -C <sub>β</sub> )	1.522	1.517	1.525	1.525	1.527	1.526	1.528	1.528
R(C <sub>β</sub> -S)	1.977	1.999	1.831	1.830	1.845	1.842	1.840	1.836
A(C <sub>α</sub> -C <sub>β</sub> -S)	109.5	107.2	110.0	113.1	110.4	113.9	109.0	104.1
R(S-N)	1.590	1.595	1.654	1.654	1.640	1.641	1.637	1.636
A(C <sub>β</sub> -S-N)	112.4	109.5	99.4	99.3	108.4	108.5	102.4	102.4
D(C <sub>α</sub> -C <sub>β</sub> -S-N)	180.0	30.8	180.0	63.8	180.0	64.8	180.0	68.1
R(N-H)			1.025	1.025	1.025	1.025	1.015	1.015
A(S-N-H)			104.9	105.1	109.8	110.1	123.1	123.2
ΔE	+0.89	0.0	+0.45	0.0	+2.61	+2.59	0.0	+0.33

<sup>a</sup> Note that the relative energies are within the same protonation state only.

**Figure 2.** Schematic structures of the lowest lying anionic (a), neutral (b), and cationic (c) forms of the sulfinylimine radicals presently investigated. Indicated are the C-C-S-N torsional angles and the spin density distribution.**Table 2.** Diagonalized Hyperfine Tensor Components<sup>a</sup> (G) for the Lowest Conformer of Each Class Listed in Table 1<sup>b</sup>

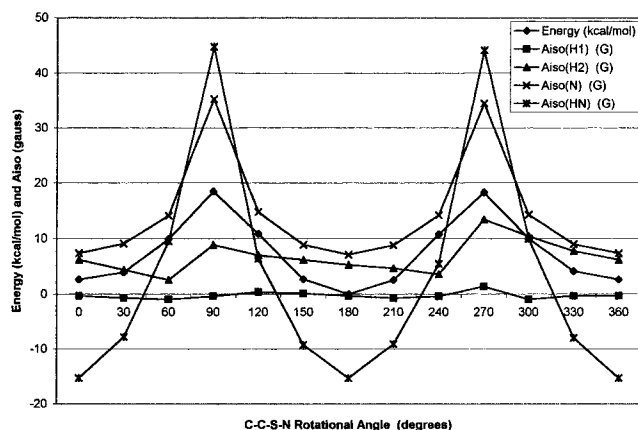
		<sup>33</sup> S	<sup>13</sup> C <sub>β</sub>	<sup>1</sup> H <sub>β1</sub>	<sup>1</sup> H <sub>β2</sub>	<sup>14</sup> N	<sup>1</sup> H(N)
R-S-N <sup>-</sup>	A <sub>xx</sub>	-10.6	-10.4	6.4	0.4	-7.3	
	A <sub>yy</sub>	-9.5	-9.3	7.0	0.5	-5.7	
	A <sub>zz</sub>	15.3	-9.0	8.8	2.2	26.3	
R-S-N-H	A <sub>xx</sub>	-9.3	-3.6	5.8	-1.0	-5.2	-21.7
	A <sub>yy</sub>	-7.7	-3.4	6.2	-1.0	-4.6	-12.0
	A <sub>zz</sub>	29.9	-3.0	8.9	1.6	26.7	4.3
R-S-N-H <sub>2</sub> <sup>+</sup>	A <sub>xx</sub>	-11.5	-3.3	13.9	13.9	-3.1	-17.1/-16.4
	A <sub>yy</sub>	-9.9	-3.0	14.6	14.6	-3.0	-10.5/-10.2
	A <sub>zz</sub>	51.3	-1.8	17.3	17.3	18.4	1.4/2.1

<sup>a</sup> Along principal magnetic axes. <sup>b</sup> Experimental Couplings: A(<sup>14</sup>N) = 25 G; A(<sup>1</sup>H<sub>β</sub>) = 6.5 G (*E. coli*) or 8–9 G (mouse).<sup>9,10</sup>

become significantly differentiated by the rotation, and we observe for both the anion and neutral systems near-zero values for the first and a tensor centered around  $7 \pm 2$  G for the second  $\beta$ -proton. This agrees closely with the experimentally observed main component for H<sub>β</sub>. Also for the nonplanar cation (not shown) a near-zero tensor is obtained for one of the protons. For the second proton, however, the tensor is considerably larger ( $A = 10.6, 11.0,$  and  $14.0$  G), and is hence too large to match the experimental data. In the case of the planar systems, the HFCCs are identical for both  $\beta$ -protons (anion, 3.9, 4.4, 6.4; trans neutral, 6.6, 7.0, 9.7; cis neutral, 7.3, 7.7, 10.3; cation, 13.9, 14.6, 17.3 G).

The nitrogen couplings are highly similar for all four neutral systems as well as for the radical anions, and have a main component of 26–27 G, in close agreement with the experimentally observed value of 25 G.<sup>9,10</sup> For the cations, on the other hand, the main component is ca. 8 G smaller, and thus deviates too much from the experimental value. From these results we can conclude that the radical species observed in the experimental work is either neutral or deprotonated. The doubly protonated form can definitely be ruled out.

It has been noted<sup>10</sup> that no imino proton could be detected in the experimental spectra. The large values of the computed hyperfine tensor for this proton in the neutral systems (Table

**Figure 3.** Relative energy (kcal/mol) and isotropic H<sub>β</sub>, N, and H<sub>N</sub> HFCCs (G) as functions of the C-S-N-H rotational angle in the neutral R-S-N-H radical.

2) could be taken as an indication of the anionic nature of the radical. However, due to the p-character of the SOMO, also the H<sub>N</sub> hyperfine components could vanish upon rotation about the S-N bond. To gain further insight into the hyperfine properties of H<sub>N</sub>, N, and H<sub>β</sub> nuclei of the neutral radical, the C-S-N-H rotational energy surface was hence investigated. The relative energies and isotropic hyperfine data, obtained by fixing the torsional angle and relaxing the remaining geometrical parameters at every 30° rotation, are displayed in Figure 3.

From these data we may conclude the following. The energetic surface displays a shallow global minimum at  $180^\circ \pm 45^\circ$  (trans), and a local minimum at  $0^\circ$  (cis) located ca. 2.5 kcal/mol higher in energy. The barrier to rotation, corresponding to breakage of the S-N  $\pi$ -bond, is substantial, and hence free rotation of the imino proton is unlikely to occur. In the energetically accessible region the isotropic H<sub>β</sub>(1), H<sub>β</sub>(2), and <sup>14</sup>N HFCCs are more or less constant at 0, 6, and  $7 \pm 1$  G, respectively. Although A<sub>iso</sub>(H<sub>N</sub>) varies more in this region, it does not vanish completely. Furthermore, the anisotropic components (-12, -3, +15 G) ensure this proton to throughout exhibit an experimentally detectable EPR component. The same conclusion applies also to the local minimum at the  $0^\circ$  rotational angle, although the energetically accessible region in this case is much more narrow.

A likely explanation may be that the sulfinylimine anion radical is formed, still interacting with the remaining substrate via H-bonding, and that this interaction keeps the substrate at the R1 active site, thereby blocking the access to the radical. Quite possibly the proton involved in H-bonding is also involved in a temperature-dependent proton-transfer equilibrium between

the sulfinylimine radical and the substrate. Once the substrate starts to decompose and the fragments diffuse out of the pocket, the radical becomes available to, e.g., water and various reactive oxygen species always present in aerobic solution, which reacts with the sulfinylimine radical in such a fashion as to destroy the cysteine and hence the protein function.

Another alternative is that the system is still bound to the sugar substrate, i.e., that a reaction has occurred by which the cysteine sulfur binds covalently to the nitrogen while this remains connected to the substrate at the C2' position. This could explain the appearance of PPI, ribose, and uracil concomitant with the decay of the sulfinylimine radical.<sup>9</sup> However, in such a case we should also be able to detect a large coupling to the remaining C2' proton (not observed). Furthermore, Salowe et al.<sup>9</sup> used <sup>13</sup>C2'-labeled ribose, but could not detect any signal from the carbon atom. This implies that the radical is not connected covalently to the modified substrate.

Given the similar nitrogen and  $\beta$ -proton HFCCs, how, then, can we differentiate between the neutral and the anionic radicals? A means to distinguish between the two possible protonation states of the sulfinylimine radical is provided from the <sup>13</sup>C $_{\beta}$  and <sup>33</sup>S HFCCs, listed in Table 2. As seen, the main component

(19) Martell, J. M.; Eriksson, L. A.; Goddard, J. D. *Acta Chem. Scand.* **1997**, *51*, 229.

on sulfur differs considerably depending on the protonation state, and could hence be used for identification purposes. However, previous studies of sulfur radical hyperfine parameters have shown that this atom poses a particularly difficult case.<sup>19</sup> Thus, a direct comparison with the presently calculated data should be made with some caution. On the other hand, the <sup>13</sup>C HFCCs are generally predicted more accurately. From Table 2 we note that these differ sufficiently between the neutral and anionic systems (-3.6, -3.4, and -3.0 G and -10.4, -9.2, and -9.0 G, respectively, at the <sup>13</sup>C $_{\beta}$  site) to allow for a unique determination of the protonation state of the radical. It is hence proposed that <sup>13</sup>C labeling at the C225 residue will be able to provide a unique determination of the protonation state of the sulfinylimine radical of azido-CDP- and azido-UDP-inhibited RNR. This may, in turn, provide valuable information regarding the reaction mechanisms proposed to occur at the active site of the enzyme.

**Acknowledgment.** This work is supported by the Swedish Natural Sciences Research Council (NFR). Professor A. Gräslund is gratefully acknowledged for valuable discussions. We also acknowledge the center for parallel computing (PDC) in Stockholm for grants of computer time.

JA973745M